Journal of Non-Crystalline Solids 357 (2011) 622–628

Contents lists available at ScienceDirect

Journal of Non-Crystalline Solids

journal homepage: www.elsevier.com/ locate/ jnoncrysol

The two-step scenario of the protein dynamical transition

W. Doster

Technische Universität München, D-85747 Garching, Physikdepartment E 13, Germany

ARTICLE INFO

Keywords:
Hydration water;
Protein dynamical transition;
Fragile-strong cross-over;
Myoglobin;
Neutron scattering

ABSTRACT

The "protein dynamical transition" (PDT) characterizes the abrupt loss of structural flexibility at a particular temperature and time scale in response to the glass transition of protein hydration water. The water-coupled structural degrees of freedom interact with the protein via hydrogen bonds, causing fluctuations, which can be probed by dynamic neutron scattering experiments. To emphasize the properties of hydration water a perdeuterated protein C–PC hydrated with H_2O is investigated together with native myoglobin. The respective intermediate scattering function of hydration water displays a two-step decay involving fast local re-orientational fluctuations and a slow collective relaxation. The anharmonic onset in the mean squared displacements, which is generally used to identify the PDT, is derived from the properties of the intermediate scattering function at the time given by the resolution of the spectrometer. It is shown that the onset temperature depends on the shape of the relaxation time spectrum. A shape-independent transition temperature T_Δ is defined, associated with the main structural relaxation, which decreases with increasing resolution. A second onset is identified near the glass temperature T_g, which is related to the initial decay of the intermediate scattering function. This onset is independent of the instrumental resolution and causes a change in molecular elasticity and thermal expansion. With this approach a more precise definition of the PDT is given, providing answers to the critical questions about the nature and the mechanism of the effect.

1. Introduction

The "protein dynamical transition" (PDT) denotes the abrupt loss of structural flexibility in response to the freezing of hydration water [1–3]. A thin layer of protein-adsorbed water remains liquid well below the freezing point and, instead of crystallizing, turns into an amorphous solid at $T_g \approx 170$ K. The term "liquid" implies viscous flow and long range diffusion in the hydration shell. The water-coupled protein degrees of freedom thus stay mobile at subzero temperatures, but become structurally arrested at T_g. These motions comprise a particular class of fluctuations, which are controlled by polar interactions, essentially by hydrogen bonds. This view is supported by molecular dynamic simulations of hydrated proteins. In particular the relevance of translational motions of water "driving" the transition was emphasized [4–6]. Internal structural degrees of freedom, side-chain rotational transitions, couple only weakly to the solvent. Such protein motions occur in spite of glassy solvents or even in the absence of solvent [7,8]. The glass transition is associated with a broad step in the specific heat of the protein–water system [1,8–11].

A second anomaly defining T_g is a discontinuity observed in the temperature dependence of the protein–water O–H stretching vibration and the peak frequencies of the amide bands [1,8,12,13]. The glass transition is phenomenologically defined by the temperature, where the structural relaxation time reaches an experimental time scale of 100 s. Probing the structural relaxation on a much shorter time scale will upshift the apparent glass temperature to T_Δ. The "Δ" indicates the dependence on the time resolution of the instrument. With Mössbauer spectroscopy on a 150 ns timescale, the transition occurs at 210 K with hydrated myoglobin [14], while probed on a 50 ps time scale with neutron scattering T_Δ is up-shifted to 240 K [2]. The protein–solvent glass transition and its effect on protein dynamics and biological function was reviewed recently in ref. [8].

The term "dynamical transition" was first introduced in the context of neutron scattering experiments performed with hydrated and dry myoglobin and lysozyme [2]. This technique records the pico-second motions of the nonexchangeable protein hydrogen atoms. A two-step scenario was already discussed in this work:"Two spectral components with different shape and temperature dependence can clearly be recognized, a fast β-process and a slower α-process. The increase with temperature of the intensity of the broad line is consistent with local jumps between sites of different energy. The linewidth is temperature independent with a value of 1.5–2 meV (0.5–1 ps). The linewidth of the α-process by contrast broadens with increasing temperature. Below 240 K this component is not well resolved and therefore contributes to the elastic intensity..." [2]. Since the slow α-process did not occur at low hydration it was assigned to collective protein–water relaxation.

In later work, the transition was predominantly identified with the "anharmonic onset" in the molecular displacements at a particular

E-mail address: wdoster@ph.tum.de.

0022-3093/$ – see front matter © 2010 Elsevier B.V. All rights reserved.
doi:10.1016/j.jnoncrysol.2010.08.002

temperature T_{on} [15]. The "onset" approach is deceptively simple, which led to a number of misconceptions[16]: Any molecular process, local or collective, can cause an apparent harmonicity transition, if probed using a fixed window method: The apparent increase of the protein NMR signal above 100–150 K due to methyl group dynamics was suggested as an explanation of the PDT [17]. Below we show, that the methyl group rotation is independent of the state of the protein environment. Often the PDT is confused with a structural phase transition, which would also modify the dynamic properties. The focus on the "anharmonic onset" has motivated other interpretations different from the glass transition scenario: (1) A sudden increase of molecular fluctuation amplitudes due to detrapping in a rugged energy landscape at $T_{on}=200$ K as observed with Mössbauer spectroscopy [18–21] or with simulations resulting from enhanced protein–water hydrogen bond dynamic amplitudes at 240 K [22]. (2) A sudden increase in protein elasticity at T_{on}, which is deduced from the change in the slope of the temperature dependent mean square displacements [23,24]. (3) A structural transition between two phases of protein hydration water [25–29]. The structural change was identified from a sharp dynamic cross-over in the temperature dependence of the average water relaxation time. We have recently shown that this cross-over results from an incomplete data analysis, when the average relaxation time of a wide spectrum crosses the instrumental resolution [13]. Also previous dielectric relaxation and NMR studies of protein hydration water could not reproduce the fragile-strong cross-over [30–33]. To clarify the issue, we briefly summarize the molecular displacements observed with myoglobin exposed to different environments.

Fig. 1 shows the mean squared amplitudes of the nonexchangeable protons of myoglobin probed on 50 ps time scale. The Q-dependent elastic n-scattering function was decomposed into two dynamic components [7]: Component I exhibits a Gaussian displacement distribution. At low temperatures this implies only vibrational motions which can be adjusted to a hyperbolic cotangent function of an average oscillator with a mean frequency of $\omega=110\ \mathrm{cm}^{-1}$. The data account correctly for the zero point vibrations. In dehydrated or glassy environments this function approximates the data quite well within the entire temperature range. In the case of D_2O-hydrated myoglobin a striking increase in the displacements occurs above 240 K due to water-coupled protein motions [2,7]. The second component was assigned to rotational transitions of side-chains, mostly of methyl groups according

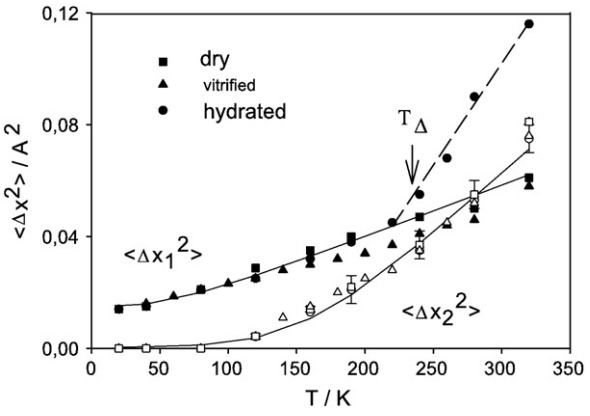

Fig. 1. Mean squared displacements of nonexchangeable hydrogen atoms of myoglobin in different environments: vacuum-dry (squares), solid, vitrified in a perdeuterated glucose glass (triangles) and liquid, D_2O-hydrated with h = 0.35 g water/g protein, (circles). The elastic neutron scattering function (IN13, ILL) was decomposed into two dynamic components: (1) Gaussian vibrational–librational displacements (filled symbols) and (2) rotational transitions of side-chains (open symbols). The full lines represent either the $\coth(\hbar\omega/k_BT)$ function (1) or a fit to a model (2), which assigns 80% of the rotational transitions to methyl groups. Only processes faster than the instrumental time resolution $\tau_\Delta\approx 50$ ps contribute to the displacements. [7,16,35].

to its non-Gaussian scattering function [7,35]. The respective anharmonic onset occurs around 150 K at $\tau_\Delta\approx 50$ ps and near 100 K at 2 ns [15]. Rotational transitions are rather unaffected by the protein environment. These motions are decoupled from the solvent and have nothing to do with the collective relaxation, which gives rise to the glass transition. The associated anharmonic onset is thus not a "dynamical transition", which involves structural arrest due to a diverging viscosity. Component I and II are not the members of the two-step scenario, mentioned in the title. The goal of this article is to identify a third dynamic component, which is closely related to the glass transition. The corresponding fluctuations of hydrogen bonds exhibit much lower amplitudes and are thus more difficult to detect by neutron scattering than the protons of rotating methyl groups. We thus analyse the fluctuations of hydration water on the surface of a protein, here the scattering from methyls has been diminished by perdeuteration as with C-phycocyanin (CPC). In a recent dynamic analysis of CPC-hydration water we recorded the temperature dependence of the average correlation time in the context of the postulated fragile to strong cross-over [13,26]. Here we focus on the properties of the elastic scattering function. We start with the theoretical background and introduce a novel approach to identify T_Δ from a neutron scattering analysis.

2. Theoretical background and data analysis of the dynamical transition

The goal of a neutron scattering experiment with proteins is to determine the self-intermediate scattering function $I(\mathrm{Q},t)$, which probes the density fluctuations of the protein hydrogens. The coherent scattering contribution due to other atoms is usually below 10%, which will be ignored in the following [34]:

$$I(\mathbf{Q},t)=\frac{1}{N}\sum_i\left\langle e^{i\mathbf{Q}\mathbf{R}_i(0)}e^{-i\mathbf{Q}\mathbf{R}_i(t)}\right\rangle \tag{1}$$

$\mathbf{R}_i(t)$ denotes the position vector of proton i at time t and $\mathbf{Q}$ is the scattering vector. N is the number of scattering centers. For isotropic samples, like protein powders, one can perform the appropriate isotropic average leading to a scalar function $I(\mathrm{Q},t)$ [7]. For Gaussian displacement distributions and finite instrumental resolution one obtains:

$$I_{app}(\mathbf{Q},t)=e^{-\frac{1}{6}\mathbf{Q}^2\left\langle\Delta R^2(t)\right\rangle}\cdot I_{res}(t/\tau_\Delta) \tag{2}$$

In general, the average squared displacement will vary with Q. The instrumental resolution function $I_{res}(t/\tau_\Delta)$ acts as a cut-off and puts a time limit on the accessible displacement. Only motions shorter τ_Δ can be observed. Most neutron scattering spectrometers provide primarily information in the frequency domain. The respective scattering function $S(\mathrm{Q},\omega)$ is given by the Fourier transform of $I(\mathrm{Q},t)$. If the value of $I(\mathrm{Q},t=\tau_\Delta)$ is finite, an apparent "elastic" scattering component with intensity $S_{app}(\mathrm{Q})$ at $\omega=0$ is produced:

$$S_{app}(\mathbf{Q},\omega=0)=\int_{-\infty}^{\infty}\frac{dt}{2\pi}I(\mathbf{Q},t)\cdot I_{res}(t/\tau_\Delta) \tag{3}$$

The measured apparent elastic intensity is usually normalized by a low temperature value $S^0_{app}(\mathrm{Q},T_0)$, where $I(\mathrm{Q},t)$ is time independent. The resulting normalized elastic intensity $S_{el}(\mathrm{Q},T,T_0)=S_{app}(\mathrm{Q},T)/S^0_{app}(\mathrm{Q},T_0)$ is the starting point of numerous neutron scattering studies with proteins aiming to derive mean squared displacements. $S_{el}(\mathrm{Q})$ has the remarkable property, that it approximates the intermediate scattering function at the resolution time τ_Δ:

$$S_{el}(\mathbf{Q},T,T_0)\approx I(\mathbf{Q},t=\tau_\Delta(T)) \tag{4}$$

This correlation is demonstrated experimentally for hydrated myoglobin in Fig. 2 on a time scale of 12 ps [37]. Note the two-step

decay of the protein intermediate scattering function first observed in 1989 [2]. By varying the instrumental resolution time τ_Δ, one can map the complete intermediate scattering function, which is discussed in Refs. [37,38]. This method establishes the connection between elastic scattering and dynamics. For the present purpose we approximate the normalized elastic intensity by the value of the intermediate scattering function at the resolution time. This ignores the detailed shape of the resolution function.

Relaxation processes in complex systems are generally non-exponential in time. A very useful model of heterogeneous processes involving a distribution of relaxation times is the Kohlrausch stretched exponential function:

$$\Phi(t) = \exp\left\{-(t/\tau_c)^{\beta}\right\} \tag{5}$$

where $\beta \leq 1$ is the stretching parameter.

Fig. 3a shows this function for various values of β. With decreasing β, the time decay broadens by fast and slow components compared to the mono-exponential case of $\beta = 1$. However, the correlation functions coincide independent of β, at $t = \tau_c$, which defines both the time scale and the characteristic temperature of the dynamical transition. The resulting "transition" in the elastic intensity $S_{el}(T)$ is shown in Fig. 3b. It was assumed that correlation time $\tau_c(T)$ varies with the temperature according to an Arrhenius law with an activation energy of 17 kJ/mol, a prefactor of 10^{-13} s (hydration water), and $\tau_\Delta = 2$ ns (HFBS, SPHERES, IN16). All curves coincide at T_Δ independent of β at $S_{el}(T_\Delta) = 1/e$, while the onset temperatures are quite different. The latter depend on the shape of the relaxation time distribution. This complication is avoided if we define the transition temperature T_Δ, by the 1/e value of the elastic intensity, where $\tau_c = \tau_\Delta$ as shown in Fig. 3b. Similarly the intermediate scattering function is characterized by its characteristic time at $t = \tau_c$ and not by the "onset" of the time decay. The elastic intensity is the primary experimental quantity and should be preferred to analysing the displacements, which involves further assumptions. Fig. 3b also illustrates, why the experimental temperature range should be chosen as wide as possible to cover the entire transition and not just the onset. The effect of a Gaussian instrumental resolution function on the elastic intensity is also shown in Fig. 3b. This produces further stretching of the high temperature tail of the elastic intensity but does not affect T_Δ [37,38]. This approach applies of course to any molecular process and not just to glassy dynamics. Molecular displacements in native proteins are spatially constrained by a compact average structure. The intermediate scattering function will therefore assume a genuine plateau at long times given by the elastic incoherent structure factor, $\mathrm{EIFS}(Q) = S_{el}(Q, \tau_\Delta \to \infty)$.

$$I_{prot}(\mathbf{Q}, t) = EISF(\mathbf{Q}) + (1 - EISF(\mathbf{Q}))\cdot\Phi_{prot}(\mathbf{Q}, t) \tag{6}$$

The EISF(Q) is defined as the Fourier transform of the displacement distribution at long times, $G(\Delta R(t \to \infty))$ and can be used to identify the type of molecular motion [7,16]. This effect, which gives rise to an elastic intensity, has to be distinguished from elastic scattering resulting from a finite instrumental resolution [7,35]. The EISF(Q), which is generally independent of the temperature, can be identified from the high temperature plateau of the elastic intensity, when the quasi-elastic spectrum is fully resolved.

We performed elastic neutron scattering experiments with perdeuterated C–PC hydrated with 0.3 g/g H_2O. C–PC is a light harvesting, blue-copper protein, abundant in blue-green algae. Its structure and dynamics have been previously investigated by neutron and X-ray scattering [34,39–41,44]. Gabel et al. have performed a very detailed neutron scattering analysis of C–PC hydration water in the presence of trehalose [42].

3. Experimental

The sample was purified from a preparation of Crespi [43,45] with nearly 99% deuteration. The protein purity was estimated from the absorbance ratio A(620 nm)/A(280 nm) ≈ 4.6 (analytical grade). The perdeuterated protein contributes essentially an elastic component, modulated by the protein structure factor [34], to the spectrum including exchanged protons (20%) and immobilized water near charged groups, from which the relevant quasi-elastic part of mobile H_2O molecules can be easily separated. The degree of hydration with H_2O was adjusted to 0.3 g/g using saturated salt solutions (KNO_3), the same hydration as in the experiments performed with lysozyme [26]. Quasi-elastic neutron scattering data were collected with the new back-scattering spectrometer SPHERES at FRM II in Munich. The standard setup with 0.65 μeV (FWHM) resolution is slightly better than with the NIST-HFBS spectrometer (0.85 μeV). Scattered neutrons were collected typically for 12 h for each spectrum in the temperature range from 100 to 320 K. The analysis was performed with the program IDA [46].

4. Results

4.1. Elastic scattering analysis of C–PC water dynamics

Fig. 4 shows an analysis of the elastic scattering function of H_2O-hydrated C–PC at a resolution time of 2 ns. Below 200 K the elastic intensity is dominated by the vibrational Debye–Waller factor. The extra loss above the onset temperature of 220 K can be attributed to an increasing resolution of the diffusional motions of hydration water [13].

The genuine elastic scattering, ≈0.25 estimated from the high temperature plateau, is dominated by coherent scattering of the protein structure, which reflects the coherent structure factor $S(Q)$ and not the EISF(Q). For mobile water one expects $\mathrm{EISF}(Q) = 0$. Taking also the vibrational component into account, yields $T_\Delta \approx 255$ K, where the correlation time of water τ_c coincides with $\tau_\Delta \approx 2$ ns. For the narrow range of the transition we assume an Arrhenius law for the average correlation time: $\langle\tau_c\rangle = \tau_0 \cdot exp(H / RT)$. The curves shown in Fig. 4 refer to two values of the stretching exponent: $\beta = 1$ (long dash) yields an activation energy of 17 kJ/mol and a pre-exponential of 10^{-13} s. The full line represents $\beta = 0.5$, yielding an activation energy of H = 33 kJ/mol (dashed 35 kJ/mol, to show the sensitivity) and the pre-exponential $\tau_0 = 10^{-15}$ s. Assuming $\beta = 0.35$, one obtains instead H = 63 kJ/mol and $\tau_0 = 10^{-22}$ s. These differences reveal the important influence of

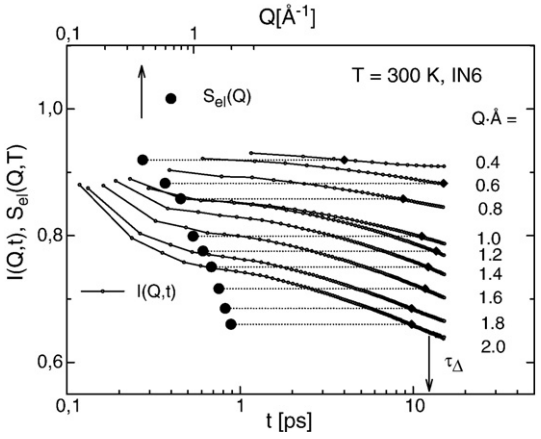

Fig. 2. Intermediate scattering function $I(Q,t)$ (corrected for resolution effects) and normalized elastic intensity $S_{el}(Q,T_0 = 100\ \mathrm{K})$ of D_2O-hydrated myoglobin (h = 0.35) measured with the time-of-flight spectrometer IN6 at the Institut Laue Langevin (Grenoble). Time window: $\tau_\Delta \approx 12$–15 ps. The horizontal lines indicate that $S_{el}(Q) = I(Q, t \approx \tau_\Delta)$.
[37,38].

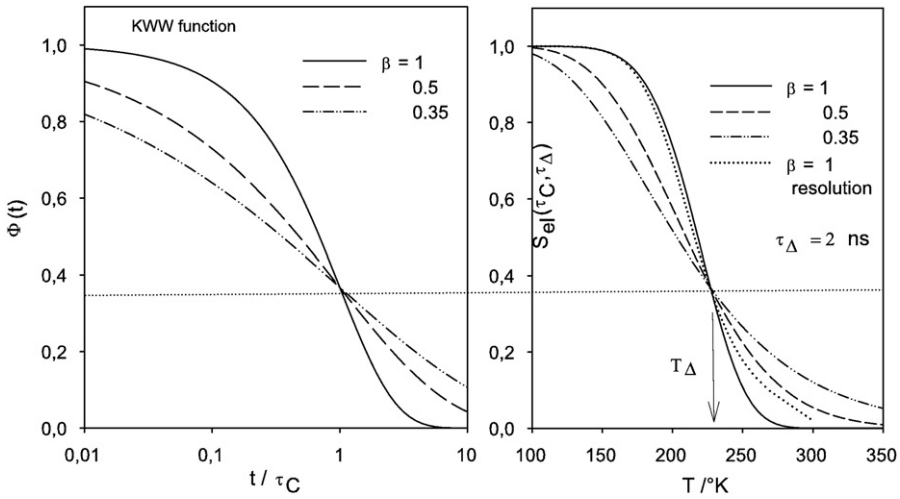

Fig. 3. a) The Kohlrausch stretched exponential function $\Phi(t/\tau_c,\beta)$ with three exponents $\beta = 0.35, 0.5, 1$. b) Resulting elastic intensity $S_{el}(T)$ at $\tau_\Delta = 2$ ns, assuming an Arrhenius law for $\tau_c(T) = \tau_0 \cdot \exp(H/RT)$ with $H = 17$ kJ/mol and a prefactor $\tau_0 = 10^{-13}$ s. The effect of a Gaussian instrumental resolution is also shown for $\beta = 1$ (dotted line) The arrow indicates the location of the dynamical transition temperature T_Δ at $\tau_\Delta = \tau_c$, independent of β.

the relaxation time distribution on the effective activation parameters. For a given β one can derive valuable dynamic information from the elastic transition curve. The average correlation times are compatible with those derived for protein hydration water by dielectric relaxation [30,31] or NMR [32,33] if a β of 0.5 is chosen. A Lorentzian, ($\beta = 1$) would not account for the wings of the C–PC water spectrum [13].

4.2. Solvent viscosity and PDT

In previous work we have introduced the viscosity near the protein surface η_s as the essential dynamic coupling parameter between the solvent and functional protein motions [7,8,14]. Moreover it was emphasized, that the viscosity near the protein surface can differ from the bulk value. The viscosity is associated with a solvent relaxation time τ_s according to the Maxwell relation. The viscosity of water has been modified in the context of neutron scattering studies with proteins by adding co-solvents at variable composition [57–59]. In the limiting case, that the relaxation rate of the bulk solvent coincides with the protein relaxation rate $\tau_c \approx \tau_s$, we can deduce from such data the corresponding PDT at a given instrumental resolution τ_Δ.

In Fig. 5 we display such results using the average solvent relaxation times given in ref. [7,8,13]. The elastic transitions occur in a temperature range of 200–300 K, consistent with published data depending on solvent composition and time window. The dashed line shows how to locate T_Δ. Hydration water as solvent at $\tau_\Delta = 140$ ns, displays the lowest onset temperature of 200 K, compatible with the 200–210 K observed in Mössbauer experiments with hydrated myoglobin [14]. This study showed in particular, that the transition temperature varies with the solvent composition and the surface viscosity. With water at 2 ns we recover the experimental results of Fig. 4. Also shown are results for 60% ethylene-glycol, 75 and 90% glycerol at a resolution of 2 ns. Note the effect of different resolution times with 90% glycerol–water at 2 and 0.1 ns. From the model discussed in Section 2 one derives the effect of viscosity on the anharmonic onset in the displacements:

$$\langle \Delta x^2 \rangle_{\tau\Delta} \approx \langle \Delta x_c^2 \rangle \left(\frac{\tau_\Delta}{\tau_c} \right)^\beta = \frac{C}{\eta^\beta} \tag{7}$$

which should be compared to the phenomenological equation $<\Delta x^2_{app}> \approx 1/\log(\eta)$ of Paciaroni et al. [58–60].

4.3. The two-step scenario

So far only the “slow” structural relaxation and the associated elastic intensity were discussed, which is the second step of a two-

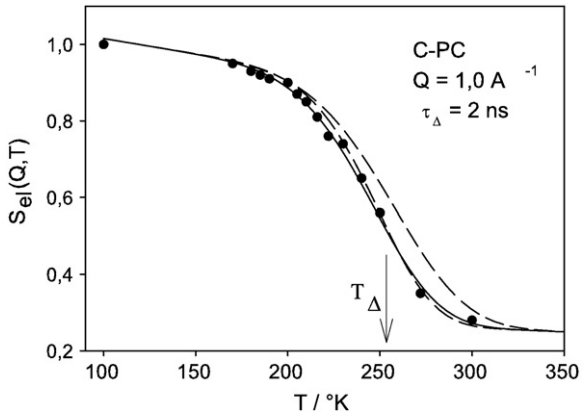

Fig. 4. Elastic neutron scattering data, $S_{el}(Q = 1.0\,\text{Å}^{-1})$ of perdeuterated phycocyanin hydrated with 0.3 g/g H_2O (filled circles). The time window was $\tau_\Delta \approx 2$ ns (SPHERES), $T_0 = 100$ K. Lines: fits to the stretched exponential model of Eqs. (5) and (6) at $\beta = 0.5$ (full line) and 1.0 (dashed). Dashed line shifted: $\beta = 0.5$ and slightly larger activation energy, T_Δ is indicated by an arrow. The parameters are given in the text.

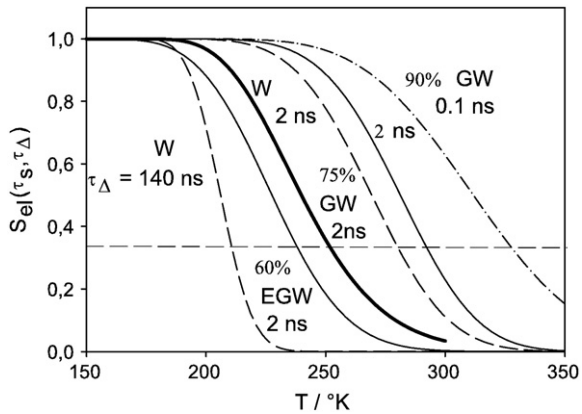

Fig. 5. Calculated elastic intensities $S_{el}(T)$ according to Eqs. (4) and (5) using the solvent relaxation times of Refs. [8,13] as input with $\tau_c = \tau_s$ and setting $\beta = 0.5$, EISF(Q) = 0. W (fat line): hydration water of Fig. 4, GW: glycerol–water in weight percent, EGW: ethylene-glycol–water. T_Δ is defined by the dashed line crossing the $S_{el}(T) = 1/e$. The instrumental resolution time windows τ_Δ are indicated.

step scenario. The first step in contrast is associated with fast hydrogen bond fluctuations and the glass transition at T_g. Fig. 6 displays the intermediate scattering function $I(Q,t)$ of protein hydration water on a 15 ps time scale corrected for resolution effects [7,8,36]. The structural correlations decay in two steps with different properties: The fast process, denoted by β, emerges with increasing amplitude at T_g. Its correlation time is nearly independent of the temperature and the wave vector Q, while the amplitude increases with Q and T. These features can be accounted for by an asymmetric two-state model of bond fluctuations [2,8].

The effective correlation time of the open-closed fluctuations is dominated by the fast crossing of the small barrier in the "excited" state. The large barrier between ground and excited state controls mainly the population of open states according to a Boltzmann distribution. This process may contain oscillatory components due to overlap with low-frequency vibrations. The second process by contrast slows down with decrease in temperature. Its rate varies with Q in accord with translational diffusion [7,36]. The slow component thus exhibits the properties expected of the α-relaxation.

The finite value of $I(Q,t=\tau_\Delta)$ gives rise to an elastic intensity as indicated in Fig. 6b. From the elastic intensity an apparent mean square displacement is deduced in the Gaussian approximation, which includes the finite time resolution of the spectrometer:

$$S_{el}(Q,T) \approx exp\left(-Q^2\left\langle \Delta x^2\right\rangle_{\tau\Delta}\right) \tag{8}$$

Fig. 7 shows the result for H_2O-CPC corresponding to a time window of 2 ns: Below 170 K the displacements are dominated by harmonic vibrational motion. Slightly above $T_g \approx 170$ K the $\langle \Delta x^2 \rangle$start to increase tending to a plateau around 200 K. A second, more striking increase occurs at $T_{on} \approx 220$ K. Fig. 7 also displays measurements of hydration water displacements, corresponding to a much shorter time window of 15 ps with hydrated myoglobin (see Figs. 3 and 5) [7]. The short-time displacements agree with the long-time measurements up to about 220 K. However $T_{on} \approx 260$ K is now upshifted by 40°. The dynamic onset thus involves two steps: A resolution-independent onset near T_g followed by a second step, where the onset temperature (T_Δ) varies with the probe frequency. Fig. 7 also shows the transition in thermal expansion coefficient of the hydrogen bond network at $T_g \approx 170$ K probed by the O–H stretching frequency shift.

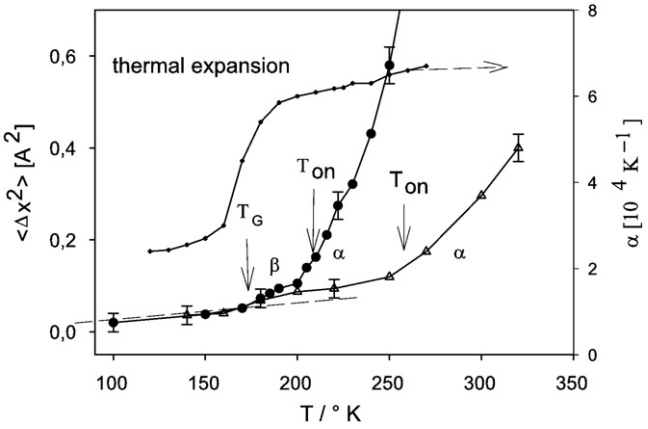

Fig. 7. Proton mean square displacements of H_2O adsorbed to C–PC at nominal time resolutions of 2 ns (full circles) and at 15 ps (open triangles, myoglobin). Dots: "Spectroscopic" thermal expansion coefficient (α) of water in hydrated myoglobin powder from the O–H stretching vibration [8,12]. The arrows locate the glass temperature T_g and the resolution-dependent onset temperatures T_{on} of the α-process. The resolution-independent onset of the fast beta-process is also marked. Dashed line: vibrational displacements.

5. Discussion

The main intention of this article is to provide an operational definition of the PDT in terms of properties of the intermediate scattering function and the physics of the glass transition. An elastic component emerges in the frequency domain, whenever $I(Q,t=\tau_\Delta)$ does not vanish within the chosen experimental time scale. If this applies to the main structural relaxation, a dynamic equilibrium cannot be achieved and the system will become nonergodic on a macroscopic scale. It was pointed out, that the decay of structural correlations requires a precursor involving local fluctuations beyond a critical amplitude. Hydration water has some dynamic features in common with the bulk phase, in particular the biphasic behavior of I(Q,t). The two-step decay in the density correlation function near the glass transition was first established by the mode coupling theory [49,50]. Its physical basis is the microscopic structure of the liquid: The fast local motions constrained by the cage of nearest neighbors give rise to a fast β-process on a pico-second time scale, while the slow α-process is associated with the escape out of the cage and long range diffusion. W. Götze in his most recent work prefers the terms "first and second scaling region" to avoid confusion with other slow β-relaxations [50].

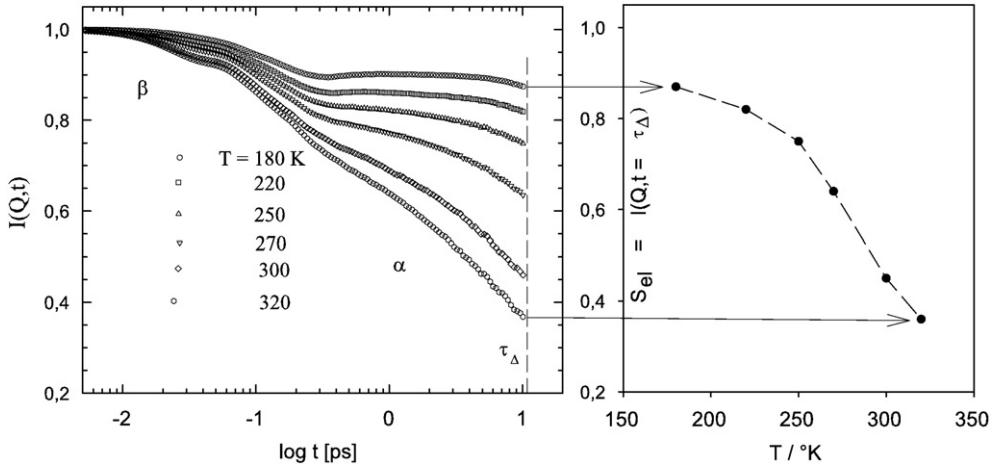

Fig. 6. Intermediate scattering function $I(Q,t)$ of hydration water of myoglobin on a 15 ps time scale at fixed $Q = 1.8\ Å^{-1}$ [7,8]. The displayed data are the result of a numerical Fourier transform of $S(Q,\omega)$ measured with instrument IN6 (ILL, Grenoble), corrected for instrumental resolution. The resulting elastic intensities at $t=\tau_\Delta$ (see the arrows) are also shown in b). The two dynamic components of $I(Q,t)$ are denoted by β and α.

Here we have shown that the biphasic behavior of $I(Q,t)$ of hydration water gives rise to two types of enhancements in the molecular displacements. The low temperature onset reflects the increasing amplitude of fast hydrogen bond fluctuations near T_g. This pre-transition leads to a change in the elasticity of the hydrogen bond network and the thermal expansion of the system. This onset cannot be observed easily with back-scattering spectroscopy of protonated proteins, because of the dominating contribution of methyl group dynamics in the same temperature range. The second step at T_Δ varies with the experimental time scale and reflects the main relaxation. This observation excludes any explanation of the PDT in terms of a structural transition as implied with the fragile-strong scenario [26]. A similar two-step increase in the displacements of hydration water can be deduced from Fig. 1 of Wood et al. with hydrated MBP, a soluble monomeric protein [47]. Also Zanotti et al. report an onset of hydration water displacements related to the calorimetric glass transition around 150–170 K with hydrated lysozyme [48]. The two-step scenario also excludes any trivial explanation of the PDT [30,51,52,54,55].

The protein–water interactions are mediated mainly by hydrogen bonding. Time-resolved displacements of protein and water protons reveal fast fluctuations on a common time scale [16]. The α-process denotes the escape of a molecule out of the cage of nearest neighbors, which is the first step of translational diffusion. The intercage displacement of water can be transmitted via hydrogen bonding to polar protein residues at the surface. This involves bond switching, since the displacements of protein residues, in contrast to water, are spatially restricted by covalent bonds. The β-relaxation discussed here is very different from the one proposed by Frauenfelder and collaborators [51]. There it is postulated that water in the hydration shell can perform only local motions. Instead water in protein powders is not attached to protein residues but performs long range diffusion as shown with NMR and neutron scattering experiments [7,13,33]. β-processes were originally introduced by Green and Angell to characterize the water-coupled motions of protein residues [56]. Their main argument, the absence of thermal effects, is however incorrect as discussed above.

Sokolov and collaborators claim, that the main protein structural relaxation and its relation to the solvent is "largely unknown" [52,53]. The connection with the glass transition of water is rejected, since the respective correlation times would not "extrapolate" to 100 s at T_g. This argument is not entirely convincing, since the glass transition of hydration water is unusually broad and new processes emerge below 210 K [30,32]. Thus the Vogel–Fulcher law observed for the average water relaxation time may not be valid below 210 K. Such a deviation from VFT behavior was indeed observed below 200 K [13,30–33]. This effect is however different from the fragile-strong cross-over proposed by Chen et al. [26] as was shown in ref. [13]. The protein anharmonicity truly increases at T_g due to enhanced fluctuation amplitudes of the H-bond network. This contrasts with the physical meaning of T_Δ, which implies $\tau_c \approx \tau_\Delta$.

6. Conclusion

The quasi-elastic neutron scattering spectrum of hydrated proteins can be decomposed into two main components: (1) Rotational transitions of side-chains, mostly of methyl groups, which are rather independent of the protein environment and (2) solvent-coupled librational motions of protein surface residues. The latter perform collective displacements in phase with water molecules near the protein surface. The intermediate scattering function of hydration water exhibits a two-step decay, similar to bulk glass-forming liquids, related to fast re-orientational and slow translational displacements. The protein dynamical transition occurs in parallel with the freezing of translational mobility of water along the protein surface. The resulting mean square displacements, measured as a function of increasing temperature, thus show a two-step onset. The onset temperature of the second step varies with the instrumental resolution time, while the first step reflecting fast hydrogen bond fluctuations is associated with enhanced amplitudes above the glass temperature T_g. The third onset, observed below T_g, refers to enhanced resolution of side-chain rotations, which are independent of the collective protein–water system. The elementary steps in the functional process of ligand binding to myoglobin show a similar behavior: The entry and exit of ligand molecules vary with the interfacial viscosity. By contrast, the protein-internal migration of ligands and the binding to the active site are completely decoupled from the solvent [7,8,16]. The protein dynamical transition (PDT) thus affects essentially the functional aspect of ligand exchange, while internal motions near the active site persist below T_g.

Acknowledgements

This article is dedicated to the numerous friends of the PDT. The author is grateful to Wolfgang Götze and to Marcus Settles for sharing their deep physical insight. Technical support with the experiments at the ILL (Grenoble) and the FRM2 (Garching) and extensive discussions with M.S. Appavou, S. Busch, A. Gaspar, J. Wuttke and H. Scheer are gratefully acknowledged. The project was supported by a grant of the Deutsche Forschungsgemeinschaft, SFB 533.

References

[1] W. Doster, T. Bachleitner, M. Hiebl, E. Lüscher, A. Dunau, Biophys. J. 50 (1986) 213.
[2] W. Doster, S. Cusack, W. Petry, Nature 337 (1989) 754.
[3] W. Doster, S. Cusack, W. Petry, Phys. Rev. Lett. 65 (1990) 1080.
[4] M. Tarek, J. Tobias, Biophys. J. 79 (2000) 3244.
[5] M. Tarek, D.J. Tobias, Phys. Rev. Lett. 88 (2002) 138101.
[6] A.L. Tournier, J. Xu, J.C. Smith, Biophys. J. 85 (2003) 1871.
[7] W. Doster, M. Settles, Biochim. Biophys. Act. 1749 (2005) 173.
[8] W. Doster, Biochim. Biophys. Act. 1804 (2010) 3.
[9] Y. Miyazaki, T. Matsuo, H. Suga, Chem. Phys. Lett. 213 (1993) 303.
[10] G. Sartor, E. Mayer, G.P. Johari, Biophys. J. 66 (1994) 249.
[11] Y. Miyazaki, T. Matsuo, H. Suga, J. Phys. Chem. B 104 (2000) 8044.
[12] F. Demmel, W. Doster, W. Petry, A. Schulte, Euro. Biophys. J. 26 (1997) 327.
[13] W. Doster, S. Busch, A.M. Gaspar, M.S. Appavou, J. Wuttke, H. Scheer, Phys. Rev. Lett. 104 (2010) 098101.
[14] H. Lichtenegger, W. Doster, T. Kleinert, B. Sepiol, G. Vogel, Biophys. J. 76 (1999) 414.
[15] J.H. Roh, V.N. Novikov, R.B. Gregory, J.E. Curtis, Z. Chowdhuri, A.P. Sokolov, Phys. Rev. Lett. 95 (2005) 038101.
[16] W. Doster, Eur. Biophys. J. 37 (2008) 591.
[17] A.L. Lee, J. Wand, Nature 411 (2001) 501.
[18] H. Frauenfelder, F. Parak, R.D. Young, Ann. Rev. Biophys. Biophys. Chem. 17 (1988) 451.
[19] H. Frauenfelder, S. Sligar, P. Wolynes, Science 254 (1991) 1598.
[20] S.H. Chong, Y. Joti, A. Kidera, N. Go, A. Ostermann, A. Gassmann, F. Parak, Eur. Biophys. J. 30 (2001) 319.
[21] F.G. Parak, K. Achterhold, S. Croci, M. Schmidt, J. Biol. Phys. 33 (2007) 371.
[22] V. Kurkal-Siebert, R. Agarwal, J.D. Smith, Phys. Rev. Lett. 100 (2008) 138102.
[23] G. Zaccai, Science 288 (2000) 1604.
[24] D.J. Bicout, G. Zaccai, Biophys. J. 80 (2001) 1115.
[25] L. Xu, P. Kumar, S.V. Buldyrev, S.H. Chen, P.H. Poole, F. Sciortino, H.E. Stanley, Proc. Natl Acad. Sci. U. S. A. 102 (2005) 16558.
[26] S.-H. Chen, L. Liu, E. Fratini, P. Baglioni, A. Faraone, A. Mamontov, Proc. Natl Acad. Sci. U. S. A. 103 (2006) 9012.
[27] S.-H. Chen, L. Liu, Y. Zang, E. Fratini, P. Baglioni, A. Faraone, A. Mamontov, J. Chem. Phys. 125 (2006) 171103.
[28] P. Kumar, G. Franzese, H.E. Stanley, Phys. Rev. Lett. 100 (2008) 105701.
[29] M. Lagi, X. Chu, Ch. Kim, F. Mallamace, P. Baglioni, S.H. Chen, J. Phys. Chem. B 112 (2008) 1571.
[30] J. Swenson, H. Jansson, R. Bergman, Phys. Rev. Lett. 96 (2006) 247802.
[31] H. Jansson, J. Swenson, Biochim. Biophys. Act. 1804 (2010) 20.
[32] M. Vogel, Phys. Rev. Lett. 101 (2008) 225701.
[33] S.A. Lusceac, M.R. Vogel, C.R. Herbers, Biochim. Biophys. Act. 1804 (2010) 41.
[34] A. Gaspar, S. Busch, M.S. Appavou, W. Haeussler, R. George, Y. Su, W. Doster, Biochim. Biophys. Act. 1804 (2010) 76.
[35] W. Doster, Physica B 835–836 (2006) 831.
[36] M. Settles, W. Doster, Faraday Disc. 103 (1996) 269.
[37] W. Doster, M. Diehl, W. Petry, M. Ferrand, Physica B 301 (2001) 65.
[38] W. Doster, M. Diehl, R. Gebhardt, R.E. Lechner, J. Pieper, Physica B 301 (2003) 65.
[39] H.D. Middendorf, Sir J. Randall, Phil. Trans. R. Soc. Lond. B 290 (1980) 639.
[40] M.C. Bellissent-Funel, J. Teixera, K.F. Bradley, S.H. Chen, J. Phys. I France 2 (1992) 995.

[41] I. Köper, S. Combet, W. Petry, M.C. Bellissent-Funel, Euro. Biophys. J. 53 (2007) 37.
[42] F. Gabel, M.C. Bellissent-Funel, Biophys. J. 92 (2007) 4054.
[43] K.F. Bradley, S.H. Chen, M.C. Bellissent-Funel, H.L. Crespi, Biophys. Chem. 53 (1994) 37.
[44] T. Schirmer, W. Bode, R. Huber, J. Mol. Biol. 196 (1987) 677.
[45] H.L. Crespi, Stable Isotopes in the Life Sciences, IAEA, Vienna, 1977, p. 111.
[46] J. Wuttke Z. Phys. Chem. (2010) submitted for publication.
[47] K. Wood, A. Frolich, A. Paciaroni, M. Moulin, M. Hertlein, G. Zaccai, D.J. Tobias, J. Am. Chem. Soc. 130 (2008) 4586.
[48] J.M. Zanotti, G. Gibrat, M.-C. Bellissent Funel, Phys. Chem. Chem. Phys. 10 (2008) 4865.
[49] W. Götze, L. Sjögren, Rep. Prog. Phys. 55 (1992) 241.
[50] W. Götze, Int. Ser. Mon. Phys.: Complex Dynamics of Glass-forming Liquids, Oxford Science Publications, 2009.
[51] P.W. Fenimore, H. Frauenfelder, B.H. McMahon, R. Young, Proc. Natl Acad. Sci. U.S.A. 10 (2004) 14408.
[52] S. Khodadadi, J.H. Roh, V.G. Sakai, E. Mamontov, A.P. Sokolov, J. Chem. Phys. 128 (2008) 1951061.
[53] S. Khodadadi, A. Malkovskiy, A.P. Sokolov, Biochim. Biophys. Acta 1804 (2010) 15.
[54] G. Chen, P.W. Fenimore, H. Frauenfelder, F. Mezei, J. Swenson, R.D. Young, Phil. Magn. 88 (2008) 3877.
[55] R.M. Daniel, J.L. Finney, J.C. Smith, Faraday Disc. 122 (2003) 163.
[56] J.L. Green, J. Fan, C.A. Angell, Phys. Chem. 98 (1994) 13780.
[57] A.M. Tsai, D.A. Neumann, L.N. Bell, Biophys. J. 79 (2000) 2728.
[58] A. Paciaroni, S. Cinelli, G. Onori, Biophys. J. 83 (2002) 1157.
[59] E. Cornicchi, M. Maroni, G. Onori, A. Paciaroni, Biophys. J. 91 (2006) 289.
[60] E. Cornicchi, G. Onori, A. Paciaroni, Phys. Rev. Lett. 95 (2005) 158104.